ORIGINAL ARTICLE

A Straightforward Approach to fNIRS Channel Selection for Distinguishing Mental States from Resting States: Effective in Both Subject-Dependent and Subject-Independent Classification Models

Ateke Goshvarpour [1, 2*]

[1] *Department of Biomedical Engineering, Imam Reza International University, Mashhad, Razavi Khorasan, Iran*

[2] *Health Technology Research Center, Imam Reza International University, Mashhad, Razavi Khorasan, Iran*

*Corresponding Author: Ateke Goshvarpour

Email: ateke.goshvarpour@gmail.com

Received: 30 January 2024 / Accepted: 20 January 2025

Abstract

Purpose: Functional Near-Infrared Spectroscopy (fNIRS) is a relatively novel tool that measures local hemodynamic changes, including oxygenated hemoglobin [Oxy-Hb], deoxygenated hemoglobin [Deoxy-Hb], and total hemoglobin [Tot-Hb]. Its safety, portability, non-invasiveness, and cost-effectiveness make it a preferred technique for designing Brain-Computer Interfaces (BCIs). This study aims to develop an accurate fNIRS-based BCI module for classifying mental tasks and the resting state.

Materials and Methods: Rather than relying on conventional statistical features, our approach utilizes nonlinear indices derived from a 2D Poincaré plot. These measures are computationally efficient and capable of revealing the underlying dynamics of the system. Our primary innovation lies in the development of a novel feature and selection method. We assessed mental task recognition in both subject-dependent and subject-independent classification modes.

Results: Our findings demonstrated a maximum accuracy of 93.75% for subject-specific style and 91.67% for subject-independent style.

Conclusion: In summary, the simplicity and high performance of the proposed framework suggest promising future directions for designing online fNIRS-based BCI systems.

Keywords: Functional Near-Infrared Spectroscopy; Poincaré Plot; Feature/Channel Selection; Mental Calculation; Classification.

DOI: https://doi.org/10.18502/fbt.v13i1.20780

1. Introduction

Brain-computer interfaces (BCIs) serve as communication tools that facilitate interaction between the human brain and external devices [1]. In recent decades, these interfaces have been the subject of extensive research, frequently by scientists. Rather than relying on the brain's natural output pathways to convey intentions, BCIs detect brain activity and convert it into control commands. As a result, they offer a potential means of communication with the external environment for individuals with movement disorders, such as paralysis or amyotrophic lateral sclerosis [2].

Researchers have utilized various neuroimaging technologies to assess cognitive load in a typical BCI due to the diverse activities occurring within the human brain. Functional Near-Infrared Spectroscopy (fNIRS) is one of the more recent neuroimaging techniques employed for functional neuroimaging. This method measures local hemodynamic changes, including levels of oxygenated hemoglobin [Oxy-Hb], deoxygenated hemoglobin [Deoxy-Hb], and total hemoglobin [Tot-Hb], by employing near-infrared light within the wavelength range of 700 to 1300 nm [3].

Although Electroencephalography (EEG), magnetoencephalography (MEG), and Event-Related brain Potentials (ERPs) exhibit high temporal resolution, they are limited by their spatial resolution. In contrast, Single-Photon Emission Computed Tomography (SPECT), Positron Emission Tomography (PET), and functional Magnetic Resonance Imaging (fMRI) are constrained by their temporal resolution. Additional limitations of these methodologies include contraindications for pediatric populations, high costs, susceptibility to movement artifacts, and restrictions on continuous or frequent measurements [3]. Conversely, fNIRS offers advantages such as safety, portability, non-invasiveness, and cost-effectiveness. Furthermore, fNIRS provides superior spatial resolution compared to EEG, better temporal resolution than fMRI, and greater resistance to electrical noise and motion artifacts than EEG [3, 4]. These benefits render fNIRS a preferred technique in the development of BCI.

A typical BCI system can be influenced by various types of mental loads to elicit brain activity. Some mental tasks are more widely studied, such as motor imagery [5-11] and mental calculations [7, 11-15], while others, including the n-back task [16-18], imagery [19], and singing a song [19], have been explored in fewer studies [19-24]. Mental calculation involves performing arithmetic operations mentally, whereas motor imagery refers to the kinesthetic visualization of one's own body organs without the engagement of muscle activity.

Recent advancements in BCI technology have been achieved through the application of neuroimaging techniques that employ a variety of protocols and signal processing methodologies. A mixed linear model for fNIRS data analysis was introduced to investigate the relationship between task difficulty and peak concentrations of [Oxy-Hb] during periods of mental effort expectation [15]. Notably, increased activity in the dorsolateral prefrontal cortex was observed in anticipation of challenging tasks compared to easier ones. However, the assessment of cerebral cortex hemodynamics was limited due to the exclusive use of frontal fNIRS channels. The system developed by Holper and Wolf [25] utilized several statistical measures derived from fNIRS data, including variance, mean amplitudes, kurtosis, and skewness, in conjunction with Fisher's linear discriminant analysis. Their objective was to distinguish between simple and complex tasks within motor imagery trials. Despite achieving an average accuracy of 81%, the limited number of experimental trials compromised the balance between accuracy rates and the number of features or trials analyzed.

FNIRS statistical measures have been employed in various studies [4, 7, 8, 10, 15, 21, 26, 27]. In their research, Hong *et al.* [7] utilized Linear Discriminant Analysis (LDA) and reported an average accuracy of 75.6% in classifying mental calculation, right-hand motor imagery, and left-hand motor imagery. However, the performance of this approach may be limited by the application of electrodes in only two specific regions of the cerebral cortex, thereby neglecting the potential contributions of other areas. In a separate study [8], the selected feature combinations were input into a hybrid genetic-SVM to identify motor imagery, achieving a subject-dependent accuracy of approximately 91%. This investigation

was constrained by the use of six statistical indices and the evaluation of only two- and three-feature fusion. Additionally, a hybrid EEG-fNIRS system [28] employed LDA attained a maximum average accuracy of 63.5% for imagery tasks and 83.6% for mental calculation. The authors attributed the low recognition rates to participants' lack of concentration during the simultaneous recording of both protocols. Aydin [27] incorporated a subject-specific feature selection algorithm within the fNIRS-BCI system, employing stepwise regression methodology based on relief F and sequential feature selection. Various machine learning algorithms were tested, resulting in a maximum accuracy of 88.67% for mental calculation using SVM and 71.32% for imagery classification using LDA. Conversely, the lowest classification rate was observed for the k-nearest neighbors (kNN) algorithm, which the authors attributed to the use of a fixed neighborhood value.

The nonlinear manifestations of brain function and concurrent metabolic processes [11], coupled with the limitations of statistical measures in adequately characterizing these phenomena, have prompted some researchers to adopt nonlinear signal analysis techniques. The study conducted was primarily exploratory and did not elucidate the neurobiological mechanisms underlying this complication. Utilizing Hilbert-based features of fNIRS in conjunction with kNN yielded a maximum accuracy of 84.94%, a sensitivity of 85.51%, and a specificity of 84.36% [29]. However, these findings were reported without a thorough investigation into the influence of classification parameters or feature selection on the performance of the system. Additionally, an independent decision path fusion methodology was proposed within a hybrid EEG-fNIRS BCI [30]. Despite the inherent complexity and the time-intensive nature of simultaneous bimodal brain data recording, the maximum accuracy achieved was 70.32%.

Previous research has predominantly focused on employing classifiers such as the hidden Markov model (HMM), SVM, LDA, and Artificial Neural Networks (ANN) [4, 7, 8, 10, 26]. Furthermore, the literature indicates that additional components may be integrated into the design of BCI systems, including preprocessing [8-11, 14, 15, 24, 26], channel selection [9, 26, 31], and feature selection [27, 32].

Our previous study encompassed various modules for a functional near-infrared spectroscopy-based brain-computer interface [33]. Initially, we proposed a subject-specific channel selection method that utilized the fNIRS energy. Subsequently, we employed a time-frequency analysis technique known as matching pursuit for feature engineering. Following this, we introduced a two-step feature selection approach that combined cascade Principal Component Analysis (PCA) with the Relief algorithm. After evaluating several classifiers, including Naïve Bayes (NB), kNN, SVM, decision tree (DT), and AdaBoost, we achieved a maximum accuracy of 86.2%. This study utilized the same data and classifiers as our previous research. The primary distinction between the current system and the previous one lies in the methodologies employed for feature engineering and channel/feature selection. Our principal contributions are outlined as follows.

(1) From the perspective of feature engineering methodologies, a majority of researchers have employed statistical analyses of fNIRS. While the computational demands of these indicators are relatively low, they are inadequate in capturing the dynamic and complex nature of brain activity. Previous studies have proposed nonlinear feature engineering techniques to address this limitation; however, many of these methods are characterized by high computational costs and complexity. In this study, we utilized phase space indicators that effectively represent system dynamics with both simplicity and rapid computational efficiency. To the best of our knowledge, no prior research has been conducted on fNIRS-based BCI analysis using the Poincaré plot.

(2) Channel and feature selection can significantly reduce the computational demands of classifiers while enhancing their performance. Previous studies have employed these approaches [8, 9, 25-27, 31-33]. However, certain methods have proven to be computationally intensive. This study proposes a novel method that is computationally efficient and has the potential to enhance the system's performance.

(3) In a limited number of studies, only subject-dependent or subject-independent channel selection methods have been implemented [8, 27, 33]. This research aims to evaluate both channel selection modes and to determine whether their outcomes are

identical or exhibit negligible or significant differences.

The subsequent sections of this study encompass the following components. The proposed methodology, which includes the fNIRS protocol and dataset, as well as the features, feature/channel selection methods, and classification techniques, is detailed in the Materials and Methods section. The Results section presents the findings, including a comparative analysis of the performance of various schemes. Finally, the Discussion and Conclusion sections synthesize the insights derived from the study.

2. Materials and Methods

Figure 1 presents a schematic representation of the proposed procedure. The system comprises several modules, including (1) fNIRS data, (2) segmentation, (3) feature engineering, (4) feature and channel selection, (5) normalization, and (6) classification. Each module is elaborated upon in the subsequent sections.

2.1. fNIRS Data

This experiment used fNIRS data from BNCI-Horizon 2020 databank, which is publicly accessible at http://bnci-horizon-2020.eu/database/data-sets. The signals were recorded while participants engaged in mental arithmetic tasks. The study included five female and three male participants, with a mean age of 26 ± 2.8 years [12]. All participants were healthy right-handed individuals, exhibiting antagonist hemodynamic response patterns during the task [12].

The experiment commenced with a ten-second baseline recording, which was subsequently followed by a mental task. Participants were required to sequentially subtract a one-digit number from a two-digit integer as quickly as possible, while the initial prompt was displayed on a video monitor. This task duration was approximately 12 seconds. Following the task, a black screen was presented for a resting period

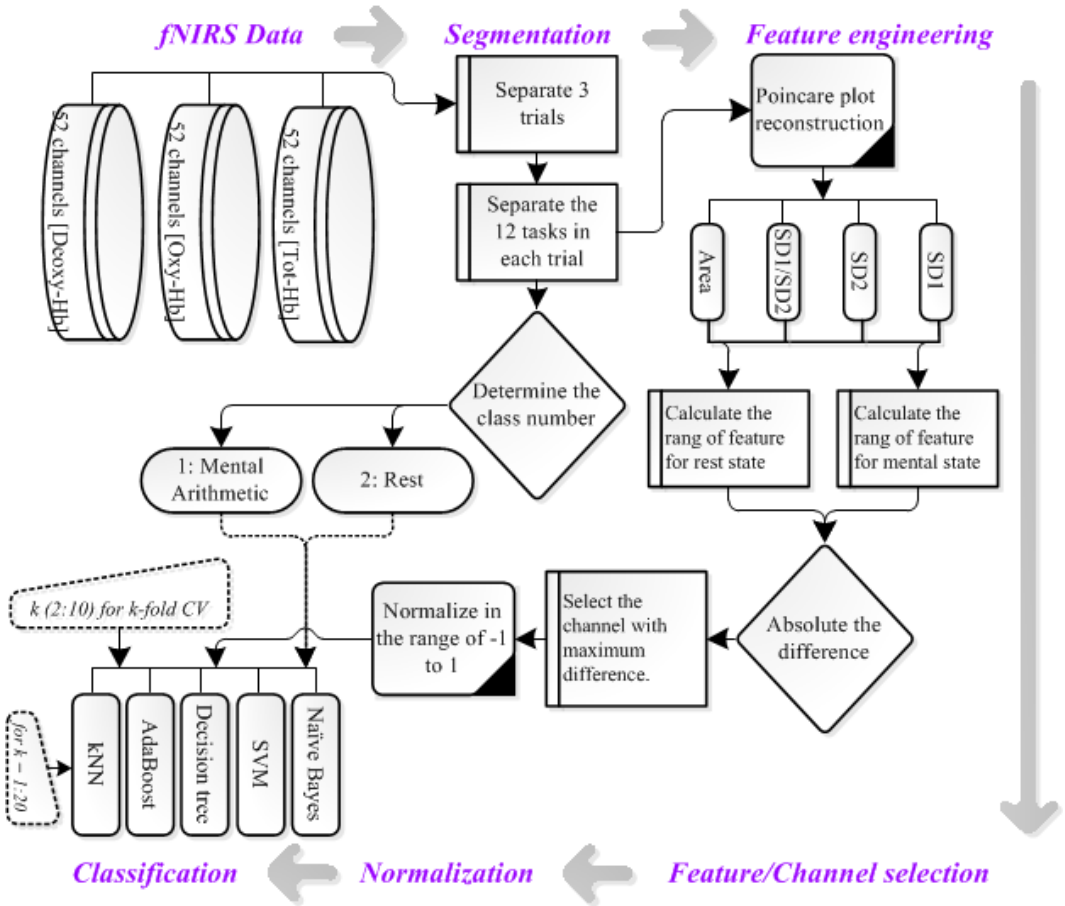

Figure 1. A schematic representation of the proposed system

of 28 seconds, during which participants were instructed to remain perfectly still and relaxed. The total duration of each trial was 40 seconds, comprising 12 seconds for the subtraction task and 28 seconds for the resting phase. Figure 2 illustrates the task schematically. Each participant completed three or four runs, encompassing a total of six trials. The present study employed three runs for all participants.

Ethical approval for the study was granted by the Institutional Review Board of the Medical University of Graz. Written informed consent was obtained from all participants after they were thoroughly informed about the study's objective. Participants were required to have no pre-existing medical conditions and were instructed to refrain from caffeine consumption before data collection. The recordings were conducted while participants were seated in a comfortable armchair, utilizing the Hitachi Medical Co. system (ETG-4000) from Japan, which is equipped with 17 light emitters and 16 photo-detectors. A 156-channel fNIRS setup was employed to measure variations of [Tot-Hb], [Oxy-Hb], and [Deoxy-Hb] expressed in millimolar × millimeter across 52 channels. The data were digitized at a sampling rate of 10 Hz.

2.2. Segmentation

Each data file is structured as a cell array with dimensions of 1 by the number of runs (3x1). The file contains the locations of the triggers in samples, labels for groups (1 indicating the mental task and 2 indicating the resting state), as well as data from 156 channels. We organized the data according to the trigger locations for each run.

2.3. Feature Engineering

A Poincaré plot serves as a straightforward method for offering a geometric representation of data within a Cartesian plane. Each point on the plot corresponds to pairs of data samples, and the distance between these points, measured in terms of the number of samples, is referred to as the lag of the plot.

Let us consider an fNIRS time series represented as X_0, X_1, …, X_N, and denotes the mean of the data. A conventional lag-1 Poincaré plot is a two-dimensional representation generated by plotting consecutive data samples (X_i, X_{i+1}). This plot serves to graphically depict the statistical correlation between successive samples. Figure 3 presents a Poincaré plot of fNIRS data, which includes 100 samples collected across two trials.

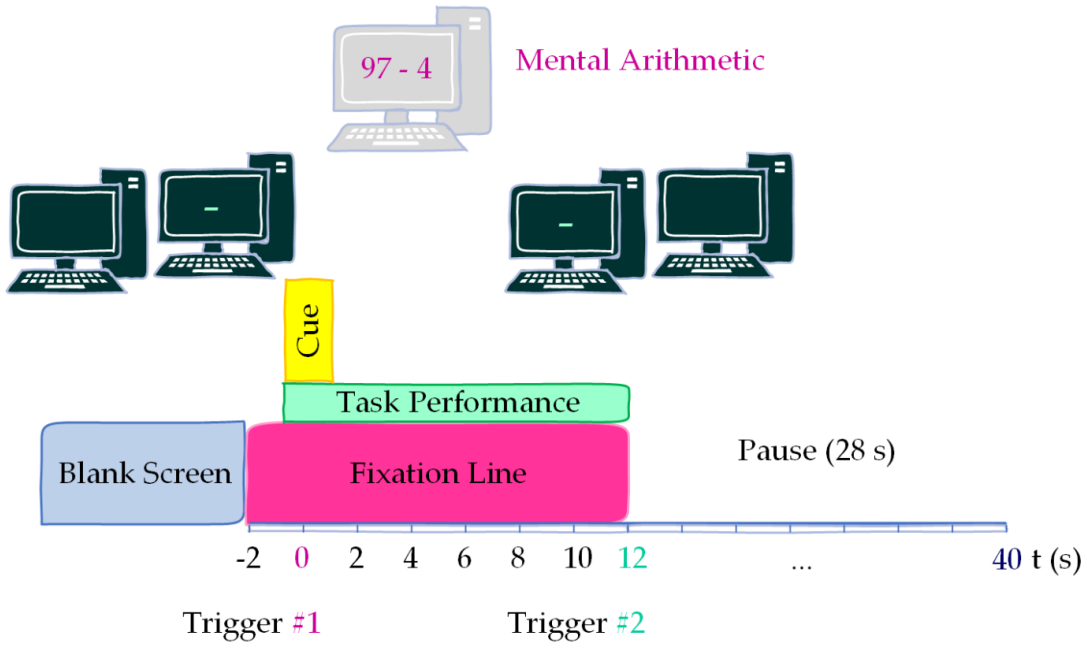

Figure 2. The temporal progression of a single trial. Two seconds before the initiation of the task, a green bar was presented. Following the cue (e.g., 97 - 4), participants were instructed to perform mental arithmetic for a duration of 12 seconds, which was subsequently succeeded by a 28-second rest period

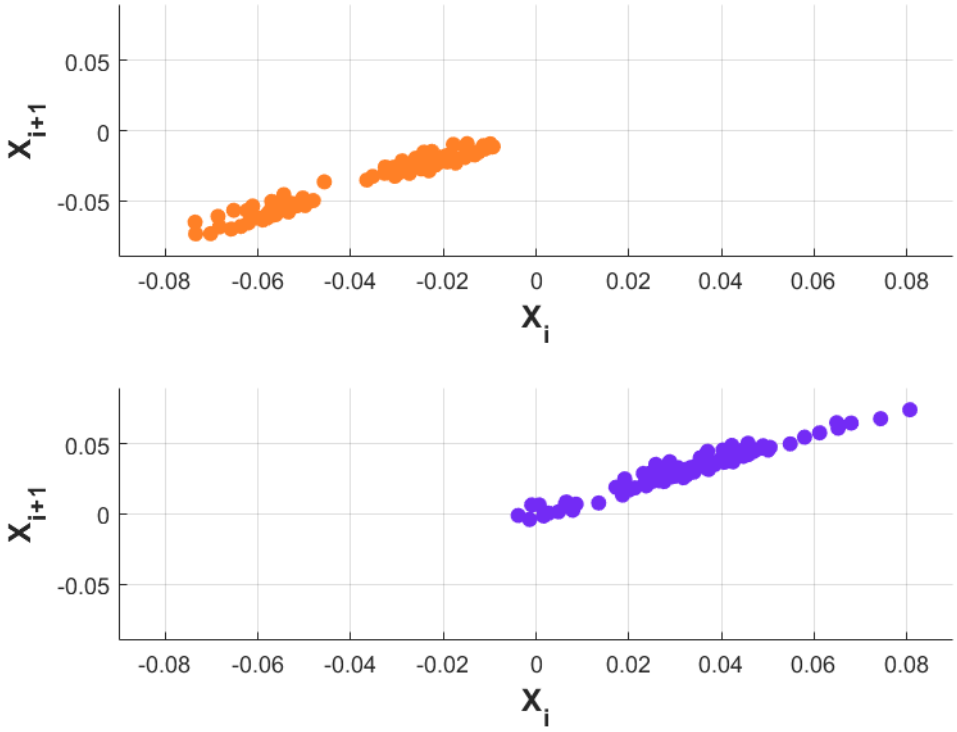

Figure 3. A sample Poincaré plot of fNIRS data from Subject 1, comprising 100 samples across two trials (top: Trial 1 and bottom: Trial 2)

A fitted ellipse is utilized in the plot to quantify the map, with the minor axis (SD1) and major axis (SD2) calculated mathematically as follows [34]:

$$SD1 = \sqrt{\frac{1}{N-1}\sum_{i=1}^{N-1\Sigma}\left(D_{i,min}\right)^2} \quad (1)$$

$$SD2 = \sqrt{\frac{1}{N-1}\sum_{i=1}^{N-1}\left(D_{i,maj}\right)^2} \quad (2)$$

The distance of the ith point on the plot from the major and minor axes can be expressed as follows.

$$D_{i,maj} = \frac{X_i + X_{i+1} - 2\bar{X}}{\sqrt{2}}, D_{i,min} = \frac{X_i - X_{i+1}}{\sqrt{2}} \quad (3)$$

The area (Ar) of the fitted ellipse is subsequently calculated according to Equation 4.

$$Ar = \pi \times SD1 \times SD2 \quad (4)$$

We also examined the ratio of SD1 to SD2 (SD1/SD2) as a quantitative measure for the plot.

2.4. Feature and Channel Selection

This experiment proposed a dual approach to channel selection, encompassing both subject-dependent and subject-independent methodologies.

Initially, the range (R = max(Y) – min(Y)) for each feature (Y) was computed across all channels under the mental task (R_m) and rest (R_r) conditions. Subsequently, the absolute value of the differences was calculated for each channel ($SC_i = |R_m - R_r|$). The channel exhibiting the maximum SC value was then identified (see Figure 4). The foundational principle of this methodology is predicated on the notion that channels demonstrating greater variability in response (i.e., broader ranges of values) are more likely to convey distinguishable information between the mental task and rest conditions. By evaluating the range of each feature for both conditions, we can determine the extent to which a channel can effectively differentiate between these states. Our approach is designed to be both subject-dependent and subject-independent, thereby enhancing its applicability across diverse individuals. By concentrating on channels with significant disparities in response ranges, we establish a flexible framework

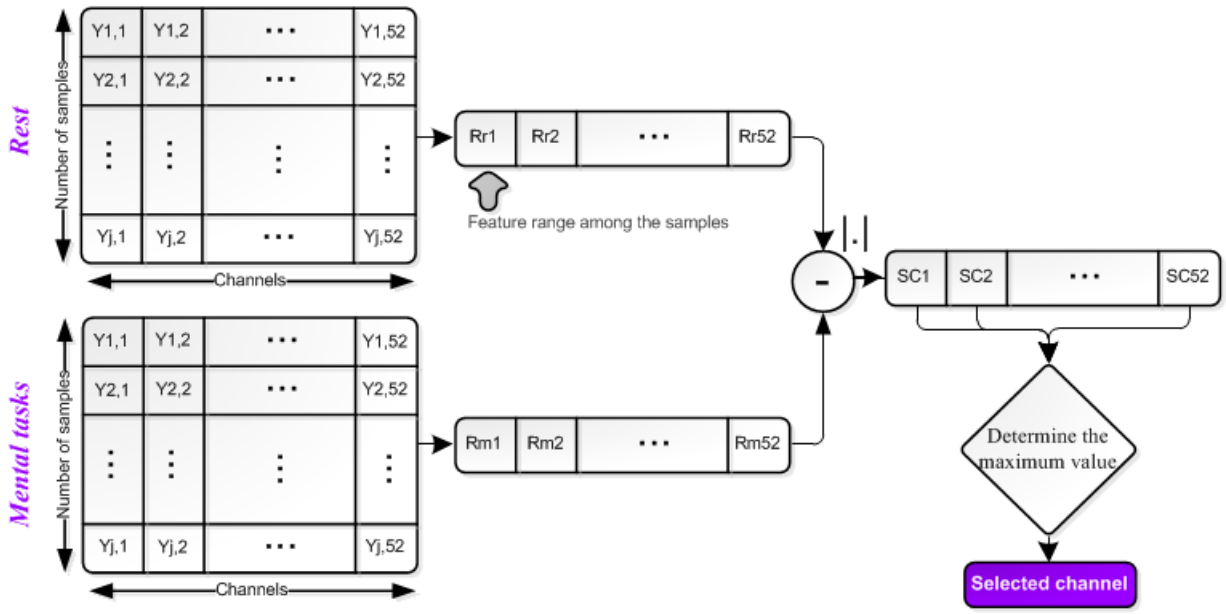

Figure 4. A typical scheme for the proposed channel selection process. The Feature values across 52 channels for each sample are represented in the matrices. The number of samples corresponding to each matrix is contingent upon the implementation of either a subject-dependent or subject-independent strategy. These matrices were generated for each of the hemodynamic features: [Oxy-Hb], [Deoxy-Hb], and [Tot-Hb]. When considering all indices of the hemodynamic responses ([Oxy-Hb], [Deoxy-Hb], and [Tot-Hb]), the total number of channels, which corresponds to the number of columns in the matrices, amounts to 156 (calculated as 52 multiplied by 3 features)

for feature selection that accommodates individual variability while simultaneously strengthening the overall analysis.

Figure 5a illustrates the selected channel from the fNIRS channels for each participant, indicating a subject-dependent selection. Conversely, Figure 5b presents the selected channel from the fNIRS channels applicable to all participants, reflecting a subject-independent selection.

It is noteworthy that, in the subject-independent mode, the selected channel for both [Oxy-Hb] and [Deoxy-Hb] remained consistent, irrespective of the type of feature utilized. In contrast, this consistency was not observed in the subject-dependent mode.

2.5. Normalization

Prior to inputting the feature vector (FV) into the classifier, it was normalized to a range of -1 to 1 using the following method.

$$Normalized \quad FV = 2\left(\frac{FV - FV_{min}}{FV_{max} - FV_{min}}\right) - 1 \qquad (5)$$

he maximum and minimum values of the FV are represented by F_{max} and F_{min}, respectively.

Data normalization constitutes an essential preprocessing step that entails the transformation of features to a uniform range, thereby mitigating the influence of larger numeric feature values on those with smaller values. The principal aim of normalization is to reduce the bias associated with features that possess a greater numerical impact in differentiating between pattern classes [35]. In the absence of normalization, the performance of the method may be negatively impacted. Features characterized by larger scales may obscure those with smaller scales, resulting in biased classification results.

The hemodynamic response features, including [Oxy-Hb], [Deoxy-Hb], and [Tot-Hb], as well as their combinations, were incorporated into the classification module.

2.6. Classification

The objective of this study was to classify two distinct conditions: "rest" and "task." We evaluated several classification algorithms, including Support Vector Machine (SVM) utilizing a radial basis function (RBF) kernel, AdaBoost, Naïve Bayes (NB),

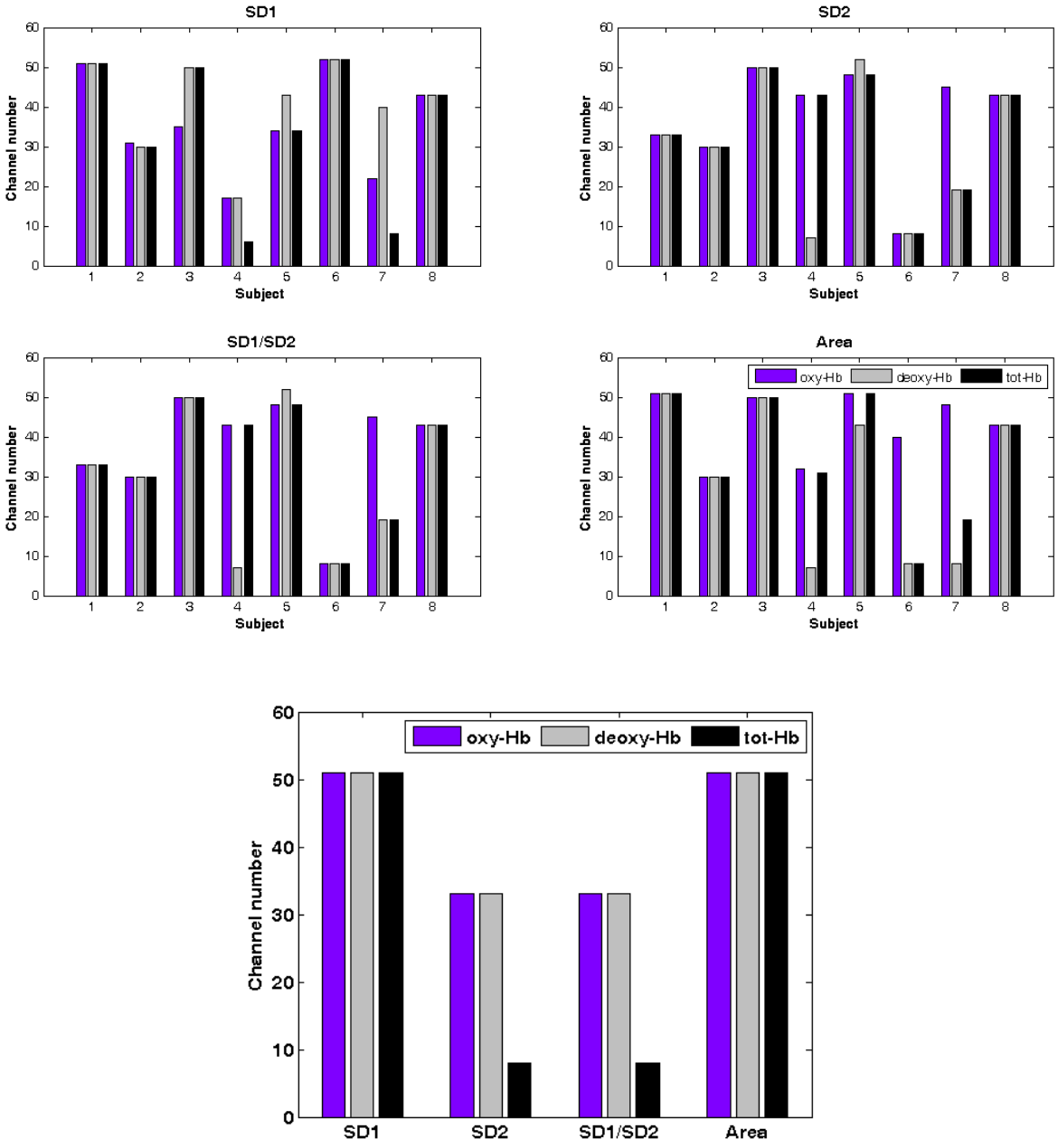

Figure 5. Selected channels for measurements of [Oxy-Hb], [Deoxy-Hb], and [Tot-Hb] in (a) subject-dependent mode and (b) subject-independent mode

Decision Tree (DT), and K-Nearest Neighbor (kNN) with varying values of k ranging from 1 to 20.

The classifiers were assessed using several performance metrics, including accuracy (AC), specificity (SP), sensitivity (SE), and F1-score (F1), employing a k-fold cross-validation (CV) approach with k values ranging from 2 to 10. The evaluation criteria were computed based on the definitions of true positive (TP), true negative (TN), false positive (FP), and false negative (FN)as follows:

$$AC(\%) = \frac{TP + TN}{TP + TN + FP + FN} \times 100 \quad (6)$$

$$SE(\%) = \frac{TP}{TP + FN} \times 100 \quad (7)$$

$$SP(\%) = \frac{TN}{TN + FP} \times 100 \quad (8)$$

$$F_1(\%) = \frac{2TP}{2TP + FP + FN} \times 100 \quad (9)$$

3. Results

Poincaré quantifiers were computed for two conditions: mental tasks and rest. Following the confirmation of normal distribution of the features via the Anderson-Darling test, we evaluated significant differences between the groups using the t-test. Table 1 presents the mean and standard deviation of the Poincaré measures, along with the corresponding statistical results.

A notable increase in the parameters SD1, SD2, and the ratio SD1/SD2 is observed in response to [Oxy-Hb] and [Deoxy-Hb], with statistical significance indicated by $p < 0.05$. Furthermore, all Poincaré indices demonstrate significant differences ($p < 0.05$) for [Tot-Hb].

Table 2 presents the highest classification results for each hemodynamic response and feature in a subject-independent mode. Furthermore, it details the classification performance when all hemodynamic responses are simultaneously input into the classifier. Specifically, the table delineates the classification outcomes for various hemodynamic responses, including Oxy-Hb, Deoxy-Hb, and Tot-Hb, utilizing different Poincaré measures such as SD1, SD2, SD1/SD2, and Area, in conjunction with high-performance classifiers. The metrics reported include Accuracy (AC), Sensitivity (SE), Specificity (SP), and F1 score (F1). Sensitivity (SE) quantifies the proportion of actual positives (task-related responses) that are correctly identified by the classifier, whereas Specificity (SP) assesses the proportion of actual negatives (rest-related responses) that are correctly recognized.

The table highlights the effectiveness of the measures, revealing that the combination of [Oxy-Hb] with the SD1/SD2 Poincaré measure using the Naïve Bayes classifier achieved the highest accuracy (85.71%) and a remarkable sensitivity of 100%, indicating that all task-related responses were correctly identified. Similarly, for [Deoxy-Hb], the SD1/SD2 measure also yielded a high accuracy of 87.50% with perfect specificity. In contrast, [Tot-Hb] showed the best performance with the SD1/SD2 measure utilizing the Naïve Bayes classifier, achieving an impressive accuracy of 91.67%, a sensitivity of 100%, a specificity of 94.12%, and an F1 score of 91.89%. Furthermore, when assessing the classification performance across all hemodynamic responses, the results indicated a slight decline in accuracy and sensitivity, with the SD2 measure still maintaining a commendable performance with an accuracy of 85.71% and a sensitivity of 81.25%. The specificity remained notably high across various classifiers and hemodynamic responses, particularly for the [Deoxy-Hb], [Tot-Hb], and all measures, which reached 100% in several instances.

Table 2 also indicates that Naïve Bayes and kNN classifiers outperformed the other classifiers, achieving the highest performance metrics. It is important to note that the classification results were significantly influenced by the choice of k-value for both the kNN and the k-fold CV.

Table 3 presents the optimal classification performance for each hemodynamic response and

Table 1. The average and standard deviation (Mean ± STD) of the features, along with the results of the t-test conducted between the two groups for various hemodynamic responses

Hemodynamic response	Poincare measures	Task	Rest	p-value
[Oxy-Hb]	SD1	0.0028±0.0049	0.0017±0.001	0.009*
	SD2	0.098±0.15	0.062±0.065	0.0014*
	SD1/SD2	0.098±0.147	0.062±0.065	0.0014*
	Area	0.0024±0.015	0.0003±0.0005	0.08
[Deoxy-Hb]	SD1	0.0017±0.0024	0.0012±0.0009	0.004*
	SD2	0.062±0.08	0.031±0.028	1.13×10^{-7}*
	SD1/SD2	0.062±0.08	0.031±0.028	1.13×10^{-7}*
	Area	0.0007±0.003	0.00015±0.0003	0.05
[Tot-Hb]	SD1	0.0037±0.0072	0.0022±0.0017	0.008*
	SD2	0.065±0.083	0.036±0.024	2.43×10^{-5}*
	SD1/SD2	0.065±0.083	0.036±0.025	2.52×10^{-5}*
	Area	0.0039±0.02	0.00056±0.001	0.04*

Table 2. Classification results for a subject-independent model

Hemodynamic response	Poincare measures	High-performance classifier	K for k-fold CV	AC	SE	SP	F1
[Oxy-Hb]	SD1	18NN	2	78.13	80	76.47	77.42
	SD2	Naïve Bayes	6	80.49	100	88.89	80.95
	SD1/SD2	Naïve Bayes	9	85.71	100	91.67	86.67
	Area	19NN	8	86.21	92.31	100	85.71
[Deoxy-Hb]	SD1	17NN	6	84.38	87.50	82.35	83.87
	SD2	16NN	1	83.33	87.50	100	82.35
	SD1/SD2	11NN	5	87.50	87.50	100	87.50
	Area	20NN	6	86.21	91.67	82.35	84.62
[Tot-Hb]	SD1	17NN	8	84.38	86.67	100	83.87
	SD2	19NN	6	82.76	81.82	100	85.71
	SD1/SD2	**Naïve Bayes**	**7**	**91.67**	**100**	**94.12**	**91.89**
	Area	16NN	2	83.33	100	100	80
All	SD1	14NN	8	83.33	87.50	80	82.35
	SD2	19NN	5	85.71	81.25	100	86.67
	SD1/SD2	17	2	84.38	86.67	100	83.87
	Area	19NN	2	82.14	76.47	100	83.87

Table 3. Classification results for a subject-dependent model

Hemodynamic response	Poincare measures	High-performance classifier	K for k-fold CV	AC	SE	SP	F1
[Oxy-Hb]	SD1	11NN	2	75	73.08	77.27	76
	SD2	**20NN**	**7**	**93.10**	**87.50**	**100**	**93.33**
	SD1/SD2	**17NN**	**8**	**93.75**	**100**	**88.89**	**93.33**
	Area	AdaBoost	7	83.33	92.86	77.27	81.25
[Deoxy-Hb]	SD1	20NN	3	75.86	70	88.89	80
	SD2	14NN	2	85.37	100	76.92	83.33
	SD1/SD2	20NN	8	85.71	85.71	85.71	85.71
	Area	19NN	4	86.21	82.35	91.67	87.50
[Tot-Hb]	SD1	18NN	7	71.88	73.33	70.59	70.97
	SD2	20NN	8	93.10	92.86	93.33	92.86
	SD1/SD2	19NN	3	89.66	88.89	92.86	89.66
	Area	18NN	6	84.38	92.31	78.95	82.76
All	SD1	20NN	6	79.31	75	84.62	80
	SD2	18NN	2	90.63	100	93.33	90.91
	SD1/SD2	20NN	6	89.66	100	83.33	88
	Area	17NN	8	84.38	86.67	82.35	83.87

feature within a subject-dependent framework. Additionally, it provides classification outcomes when all hemodynamic responses are concurrently input into the classifier.

Table 3 indicates that the kNN classifier outperformed the other classifiers, achieving the highest performance metrics. However, the results were significantly influenced by the choice of the k-value for kNN and the k-value utilized for k-fold CV. When employing the [Oxy-Hb] variable, the accuracy rates attained were 93.75% and 93.1%, with an 8-fold CV applied for the SD1/SD2, and a 7-fold CV implemented for the SD2. The sensitivity, specificity, and F-score were recorded at 100%, 88.89%, and 93.33%, respectively. Furthermore, an accuracy of 93.1% was achieved when the SD2 of the Total Hemoglobin ([Tot-Hb]) was input into the 20-Nearest Neighbors (20NN) model. Among the Poincaré measures, SD2 demonstrated the highest performance, while the second-best Poincaré measure was identified as SD1/SD2.

A comparison of the results from the subject-independent (Table 2) and the subject-dependent (Table 3) indicates that the subject-dependent strategy demonstrates superior performance in classifying rest and task states.

The study employed an Intel(R) Core(TM) i7-14650HX processor with a clock speed of 2.20 GHz. The time required for subject-dependent channel selection was recorded at 0.621456 seconds, whereas the time for subject-independent channel selection was noted to be 0.560980 seconds. These findings indicate that the proposed method exhibits computational efficiency, rendering it appropriate for real-time applications. Furthermore, the straightforward nature of the channel selection algorithm reduces computational complexity, thereby enhancing its suitability for incorporation into wearable fNIRS devices.

4. Discussion

This study aims to propose an accurate fNIRS system for the classification of mental tasks and resting conditions. The primary focus is on presenting a novel and straightforward approach for channel selection, as well as evaluating the outcomes in both subject-dependent and subject-independent modes. We employed Poincaré-based indices to analyze the various hemodynamic responses. Subsequently, a channel-selection algorithm was developed, emphasizing the most significant changes in characteristics between the two states. Following the normalization of the feature vector, a decision-making module was implemented, wherein NB, DT, SVM, kNN, and AdaBoost were assessed for mental task recognition. The maximum accuracy achieved was 93.75% using a subject-specific channel selection procedure. Furthermore, our findings indicate the superiority of the kNN algorithm, particularly highlighting the importance of the k values and k-fold CV on recognition rates.

We conducted a comparative analysis of the performance of the proposed system against previously established systems, as summarized in Table 4.

Table 4 demonstrates the superiority of the current system, as evidenced by its higher classification rates in comparison to other existing models.

Most of the scientists referenced have employed conventional methodologies for statistical signal analysis [7, 8, 17, 24, 25, 27, 28, 37, 38]. In contrast, this study adopts a non-linear feature engineering approach. The methodology is based on the principles of non-linear dynamics and deterministic chaos, with a focus on characterizing system attractors and their invariant parameters [39]. The non-linear features are designed to capture complex relationships and interactions that may not be sufficiently represented by linear models [39]. This approach facilitates a more nuanced understanding of how various cognitive tasks are encoded by neural populations. Furthermore, LDA has been utilized as a classifier in the majority of the studies reviewed [7, 12, 25, 27, 28, 37, 38], yielding accuracy rates ranging from approximately 63% to 89%. However, none of these studies have provided alternative criteria for evaluating classifier performance. Additionally, our proposed system demonstrates superiority over the non-linear feature engineering system presented by Ergün and Aydemir [29]. Their study examined Hilbert-based features in conjunction with kNN, achieving maximum accuracies of 84.94% for [Oxy-Hb] and 82.87% for [Deoxy-Hb]. A self-governing decision path fusion methodology was introduced by Jiang *et al.* [30] for a hybrid EEG and fNIRS BCI, resulting in a maximum accuracy of 70.32%, which is significantly lower than the performance of our system. Another hybrid EEG-fNIRS system proposed by Li *et al.* [9] achieved the highest accuracy of 91.02%; however, this accuracy decreased to 85.55% when utilizing fNIRS alone. Recent literature has suggested the implementation of channel selection and cascade feature selection for fNIRS task recognition [33], reporting a maximum accuracy of 86.2% using matching pursuit-based indices. Although the data and classifiers employed in the present study are identical to those in previous research, our system has enhanced the maximum accuracy rate by approximately 7%.

Table 4. A comparison of the performance of the proposed system with previously presented schemes

Study	Task	No. of subjects	Feature Engineering	Classification and other procedures	Maximum accuracy (%)
[25]	Imagery	12	Skewness, kurtosis, variance, and mean signal amplitudes	Fisher's linear discriminant analysis	81
[12]	Mental calculation	8	The task-related concentration changes of [oxy-Hb] referred to a 10-s baseline interval before the task	LDA, three regions of interest	79.7
[21]	Mental workload	12	Average of [Oxy-Hb], and spectral indices of heart rate	ANOVA test	-
[7]	Mental calculation, imagery	10	Mean and slope of the signal	LDA	75.6
[31]	Mental calculation	5	3D fNIRS imaging by bundled-optode arrangement, average of [Oxy-Hb]	-	-
[28]	Mental calculation, imagery	29	Mean and slope of concentration changes of [Deoxy-Hb] and [Oxy-Hb]	LDA.	80.7[Deoxy-Hb]/83.6[Oxy-Hb] for mental calculation 66.5[Deoxy-Hb]/63.5[Oxy-Hb] for imagery
[9]	Motor task	11	A general linear model and temporal features, a hybrid EEG-fNIRS scheme	SVM	91.02 (hybrid) 85.55 (fNIRS)
[8]	Imagery	5	Slope, mean, kurtosis, peak, variance, and skewness from the [Oxy-Hb]	Hybrid genetic algorithm-SVM	91% (subject-dependent)
[29]	Mental calculation	29	Hilbert-based indices of [Oxy-Hb] and [Deoxy-Hb]	kNN	82.87 [Deoxy-Hb] 84.94 [Oxy-Hb]
[30]	Mental calculation, imagery	29	-	Independent decision path fusion of EEG and fNIRS	70.3
[27]	Mental calculation, imagery	29	Mean, slope, peak, skewness and kurtosis, of fNIRS	LDA, kNN, and SVM, sequential feature selection and reliefF	77.01[Deoxy-Hb]/71.32[Oxy-Hb] for imagery 88.67[Deoxy-Hb]/86.43[Oxy-Hb] for mental calculation
[24]	Mental workload	20	Concentration changes in [Oxy-Hb] and [Deoxy-Hb]	ANOVA, Principal Component Analysis	-
[36]	Mental calculation	8	General linear model to identify the active areas of the brain	-	-
[17]	N-back task	25	Traditional measures	ANOVA, topographic maps,	-
[37]	Mental calculation	8	Average, minimum, maximum, variance, and slope	LDA, QDA, and SVM	89.73 by QDA
[38]	Imagery	20	mean, slope, maximum of [Oxy-Hb] and minimum of [Deoxy-Hb]	Fisher score, SVM, LDA, kNN	69.6
[33]	Mental calculation	8	Matching pursuit-based indices	AdaBoost, kNN, SVM, NB, DT, channel selection, cascade feature selection	86.2 by DT
Current study	**Mental calculation**	**8**	**Poincare plot measures**	**Subject-dependent and subject-independent feature/channel selection, AdaBoost, kNN, SVM, NB, DT**	**93.75 (subject-dependent) 91.67 (subject-independent)**

The proposed system demonstrated effective performance in both subject-dependent and subject-independent feature/channel selection modes, indicating its potential for the advancement of fNIRS-BCI systems in future applications.

The methodology employed in this paper is characterized by its simplicity in terms of feature engineering and feature/channel selection, while being efficient in distinguishing between mental tasks and rest conditions. The straightforward nature of our approach presents a significant advantage for potential integration into wearable fNIRS devices. The implementation of a basic channel-selection algorithm, alongside the application of fundamental statistical measures, minimizes computational demands, thus rendering the approach suitable for real-time applications within wearable technology contexts. The capacity for real-time classification of mental tasks and rest conditions facilitates diverse practical applications, including neurofeedback, brain-computer interfaces, and cognitive state monitoring. This simplicity further enhances the adaptability of our method to lower-resolution systems. Even with diminished spatial resolution, our channel-selection strategy remains capable of effectively identifying the most informative channels, ensuring consistent classification performance.

Nevertheless, the study is not without its limitations. The restricted number of database samples poses challenges to the generalizability of the proposed algorithm. Addressing this limitation necessitates the evaluation of a broader array of fNIRS recordings. Our process of feature/channel selection was conducted to feature engineering. Future investigations might consider incorporating this step before feature extraction to enhance computational efficiency. This study establishes a straightforward feature selection criterion, utilizing the maximum range difference as the primary metric. Other metrics could yield supplementary insights; for instance, identifying channels with features highly correlated to task performance may enhance the selection of those channels that best reflect the cognitive demands of the mental task, potentially resulting in improved classification accuracy. Furthermore, by examining the spatial patterns of hemodynamic responses, it may be possible to pinpoint regions of interest consistently activated during mental tasks. Such an approach could bolster the interpretability and relevance of the selected channels, particularly in studies focusing on specific cognitive tasks. Future research should consider the exploration of alternative metrics, such as correlation with task performance or the spatial distribution of brain activity. In our analysis, we opted to utilize a singular time lag for the computation of the Poincaré plot [41]. However, the application of multiple time lags could facilitate a more nuanced understanding of data dynamics. Therefore, future investigations are warranted to systematically examine the optimal time lag for fNIRS data, potentially yielding more refined measurements of temporal variability.

Additionally, this study adhered to a binary classification framework, distinguishing between mental task and resting condition. This constraint arises from the dataset, which only provides "rest" and "task" labels, thereby limiting our exploration of multi-class classification scenarios. Further research should involve the collection of more extensive datasets that encompass multiple mental tasks or varying levels of task difficulty. Moreover, the feature selection methodology, which relies on the range and absolute differences of characteristics between the two states, would necessitate adaptation for multi-class settings. Identifying the most discriminative features across multiple classes in such scenarios could prove more complex and may require the implementation of advanced feature selection algorithms.

In our study, the kNN classifier exhibited superior performance compared to other methods, such as SVM. This variation in performance can be attributed to several factors, including the inherent characteristics of the data, the underlying assumptions associated with each classifier, and the influence of hyperparameters. For example, the choice of the k-value is critical in the kNN algorithm; a lower k-value may render the classifier susceptible to noise, whereas a higher k-value could smooth the decision boundary, possibly obscuring finer distinctions between classes [40]. Future work should incorporate a more comprehensive hyperparameter optimization strategy for the classifiers. Additionally, exploring ensemble methods that amalgamate multiple classifiers may further enhance performance by capitalizing on the strengths of each approach.

5. Conclusion

Recent advancements in the development of fNIRS-based BCI systems have led to a significant increase in interest aimed at creating user-friendly and naturalistic communication schemes. In this context, we have proposed a novel and straightforward tool for the classification of mental arithmetic tasks. Contrary to conventional methodologies that primarily utilize statistical features, our approach employs nonlinear indices derived from two-dimensional phase space. These features, while computationally simple, effectively elucidate the dynamics of the system. A key innovation of our procedure is the introduction of a new feature/channel selection strategy, which we evaluated in both subject-dependent and subject-independent classification modes. Despite the computational simplicity of our method, the results obtained in both modes were notably impressive. The rapid and uncomplicated calculations offered by the proposed algorithm, along with its high performance in differentiating between mental states, position it as a promising candidate model for the development of online fNIRS-BCI systems.

Acknowledgements

I would like to extend my sincere appreciation to my sister, Dr. Atefeh Goshvarpour, who has provided unwavering inspiration and guidance throughout my educational and academic pursuits. Her expertise and advice have been invaluable in shaping my understanding of the subject matter and have contributed significantly to my ability to write the articles. I am grateful for her support and mentorship, and I would like to acknowledge her role in helping me to develop my skills and knowledge, and thank her for her invaluable contributions to my personal and professional growth.

References

1- Wolpaw, J. R., Birbaumer, N., McFarland, D. J., Pfurtscheller, G., & Vaughan, T. M. "Brain-computer interfaces for communication and control. Clinical neurophysiology." *official journal of the International Federation of Clinical Neurophysiology*, 113(6), 767–791, (2002). https://doi.org/10.1016/s1388-2457(02)00057-3

2- van Gerven M, Farquhar J, Schaefer R, Vlek R, Geuze J, Nijholt A, Ramsey N, Haselager P, Vuurpijl L, Gielen S, Desain P. "The brain-computer interface cycle." *J Neural Eng*.;6(4):041001, (2009). doi: 10.1088/1741-2560/6/4/041001.

3- Irani, F., Platek, S. M., Bunce, S., Ruocco, A. C., & Chute, D. "Functional near-infrared spectroscopy (fNIRS): an emerging neuroimaging technology with important applications for the study of brain disorders." *The Clinical neuropsychologist*, 21(1), 9–37, (2007). https://doi.org/10.1080/13854040600910018

4- Naseer, N., & Hong, K. S:"fNIRS-based brain-computer interfaces: a review." *Frontiers in human neuroscience*, 9, 3, (2015). https://doi.org/10.3389/fnhum.2015.00003

5- Beisteiner, R., Höllinger, P., Lindinger, G., Lang, W., & Berthoz, A. "Mental representations of movements. Brain potentials associated with the imagination of hand movements." *Electroencephalography and clinical neurophysiology*, 96(2), 183–193, (1995). https://doi.org/10.1016/0168-5597(94)00226-5

6- Sitaram, R., Zhang, H., Guan, C., Thulasidas, M., Hoshi, Y., Ishikawa, A., Shimizu, K., & Birbaumer, N. "Temporal classification of multichannel near-infrared spectroscopy signals of motor imagery for developing a brain-computer interface." *NeuroImage*, 34(4), 1416–1427 , (2007). https://doi.org/10.1016/j.neuroimage.2006.11.005

7- Hong, K. S., Naseer, N., & Kim, Y. H. "Classification of prefrontal and motor cortex signals for three-class fNIRS-BCI." *Neuroscience letters*, 587, 87–92, (2015). https://doi.org/10.1016/j.neulet.2014.12.029

8- Noori, F. M., Naseer, N., Qureshi, N. K., Nazeer, H., & Khan, R. A. "Optimal feature selection from fNIRS signals using genetic algorithms for BCI." *Neuroscience letters*, 647, 61–66, (2017). https://doi.org/10.1016/j.neulet.2017.03.013

9- Li, R., Potter, T., Huang, W., & Zhang, Y. "Enhancing Performance of a Hybrid EEG-fNIRS System Using Channel Selection and Early Temporal Features." *Frontiers in human neuroscience*, 11, 462, (2017). https://doi.org/10.3389/fnhum.2017.00462

10- Ghaffar, M.S.B.A., Khan, U.S., Iqbal, J., Rashid, N., Hamza, A., Qureshi, W.S., Tiwana, M.I., Izhar, U. "Improving classification performance of four class FNIRS-BCI using Mel Frequency Cepstral Coefficients (MFCC)." *Infrared Physics & Technology*, 112, 103589, (2021). https://doi.org/10.1016/j.infrared.2020.103589.

11- Ghouse, A., Nardelli, M., & Valenza, G. "fNIRS Complexity Analysis for the Assessment of Motor Imagery and Mental Arithmetic Tasks." *Entropy (Basel, Switzerland)*, 22(7), 761, (2020). https://doi.org/10.3390/e22070761

12- Bauernfeind, G., Scherer, R., Pfurtscheller, G., & Neuper, C. "Single-trial classification of antagonistic oxyhemoglobin responses during mental arithmetic."

Medical & biological engineering & computing, 49(9), 979–984, (2011). https://doi.org/10.1007/s11517-011-0792-5

13- Bauernfeind, G., Steyrl, D., Brunner, C., & Muller-Putz, G. R. "Single-trial classification of fNIRS-based brain-computer interface mental arithmetic data: a comparison between different classifiers." *Annual International Conference of the IEEE Engineering in Medicine and Biology Society*, 2004–2007, (2014). https://doi.org/10.1109/EMBC.2014.6944008

14- Kurz, E. M., Wood, G., Kober, S. E., Schippinger, W., Pichler, G., Müller-Putz, G., & Bauernfeind, G. "Towards using fNIRS recordings of mental arithmetic for the detection of residual cognitive activity in patients with disorders of consciousness (DOC)." *Brain and cognition*, 125, 78–87, (2018). https://doi.org/10.1016/j.bandc.2018.06.002

15- Vassena, E., Gerrits, R., Demanet, J., Verguts, T., & Siugzdaite, R. "Anticipation of a mentally effortful task recruits Dorsolateral Prefrontal Cortex: An fNIRS validation study." *Neuropsychologia*, 123, 106–115, (2019). https://doi.org/10.1016/j.neuropsychologia.2018.04.033

16- Herff, C., Heger, D., Fortmann, O., Hennrich, J., Putze, F., & Schultz, T. "Mental workload during n-back task-quantified in the prefrontal cortex using fNIRS." *Frontiers in human neuroscience*, 7, 935, (2014). https://doi.org/10.3389/fnhum.2013.00935

17- Saikia, M. J., Besio, W. G., & Mankodiya, K. "The Validation of a Portable Functional NIRS System for Assessing Mental Workload." *Sensors (Basel, Switzerland)*, 21(11), 3810, (2021). https://doi.org/10.3390/s21113810

18- Shirzadi, S., Einalou, Z., & Dadgostar, M. "Investigation of Functional Connectivity During Working Memory Task and Hemispheric Lateralization in Left- and Right-Handers Measured by fNIRS." *Optik*, 221: 165347, (2020). https://doi.org/10.1016/j.ijleo.2020.165347.

19- Naito, M., Michioka, Y., Ozawa, K., Ito, Y., Kiguchi, M., Kanazawa, T. (2007). "A communication means for totally locked-in ALS patients based on changes in cerebral blood volume measured with near-infrared light." *IEICE Transactions on Information and Systems*, E90D(7), 1028-1037, (2007). doi:10.1093/ietisy/e90-d.7.1028

20- Putze, F., Hesslinger, S., Tse, C. Y., Huang, Y., Herff, C., Guan, C., & Schultz, T. "Hybrid fNIRS-EEG based classification of auditory and visual perception processes." *Frontiers in neuroscience*, 8, 373, (2014). https://doi.org/10.3389/fnins.2014.00373

21- Durantin, G., Gagnon, J. F., Tremblay, S., & Dehais, F. "Using near infrared spectroscopy and heart rate variability to detect mental overload." *Behavioral brain research*, 259, 16–23, (2014). https://doi.org/10.1016/j.bbr.2013.10.042

22- Invitto, S., Montinaro, R., Ciccarese, V., Venturella, I., Fronda, G., & Balconi, M. "Smell and 3D Haptic Representation: A Common Pathway to Understand Brain Dynamics in a Cross-Modal Task." *A Pilot OERP and fNIRS Study. Frontiers in behavioral neuroscience*, 13, 226, (2019). https://doi.org/10.3389/fnbeh.2019.00226

23- Abdalmalak, A., Milej, D., Norton, L., Debicki, D. B., Owen, A. M., & Lawrence, K. S. "The Potential Role of fNIRS in Evaluating Levels of Consciousness." *Frontiers in human neuroscience*, 15, 703405, (2021). https://doi.org/10.3389/fnhum.2021.703405

24- Midha, S., Maior, H.A., Wilson, M.L., & Sharples, S. "Measuring Mental Workload Variations in Office Work Tasks using fNIRS." *International Journal of Human-Computer Studies*, 147, 102580, (2021). https://doi.org/10.1016/j.ijhcs.2020.102580.

25- Holper, L., & Wolf, M. "Single-trial classification of motor imagery differing in task complexity: a functional near-infrared spectroscopy study." *Journal of neuro engineering and rehabilitation*, 8, 34, (2011). https://doi.org/10.1186/1743-0003-8-34

26- Khan, M. J., & Hong, K. S. "Passive BCI based on drowsiness detection: an fNIRS study." *Biomedical optics express*, 6(10), 4063–4078, (2015). https://doi.org/10.1364/BOE.6.004063

27- Aydin E. A. "Subject-Specific feature selection for near infrared spectroscopy-based brain-computer interfaces." *Computer methods and programs in biomedicine*, 195, 105535, (2020). https://doi.org/10.1016/j.cmpb.2020.105535

28- Shin, J., von Luhmann, A., Blankertz, B., Kim, D. W., Jeong, J., Hwang, H. J., & Muller, K. R. "Open Access Dataset for EEG+NIRS Single-Trial Classification. ", *IEEE transactions on neural systems and rehabilitation engineering: a publication of the IEEE Engineering in Medicine and Biology Society*, 25(10), 1735–1745, (2017). https://doi.org/10.1109/TNSRE.2016.2628057

29- Ergün E., & Aydemir, Ö. "Decoding of Binary Mental Arithmetic Based Near-Infrared Spectroscopy Signals." *3rd International Conference on Computer Science and Engineering (UBMK)*, 2018, 201-204, (2018). doi: 10.1109/UBMK.2018.8566462.

30- Jiang, X., Gu, X., Xu, K., Ren, H., & Chen, W. "Independent Decision Path Fusion for Bimodal Asynchronous Brain–Computer Interface to Discriminate Multiclass Mental States." *IEEE Access*, 7, 165303-165317, (2019). doi: 10.1109/ACCESS.2019.2953535.

31- Nguyen, H. D., & Hong, K. S. "Bundled-optode implementation for 3D imaging in functional near-infrared spectroscopy." *Biomedical optics express*, 7(9), 3491–3507, (2016). https://doi.org/10.1364/BOE.7.003491

32- Naseer, N., Noori, F. M., Qureshi, N. K., & Hong, K. S. "Determining Optimal Feature-Combination for LDA Classification of Functional Near-Infrared Spectroscopy

Signals in Brain-Computer Interface Application." *Frontiers in human neuroscience*, 10, 237, (2016). https://doi.org/10.3389/fnhum.2016.00237

33- Goshvarpour A, Goshvarpour A. "Matching pursuit-based analysis of fNIRS in combination with cascade PCA and reliefF for mental task recognition. ", *Expert Systems with Applications 2023; 213(Part C*): 119283. https://doi.org/10.1016/j.eswa.2022.119283

34- Khandoker AH, Karmakar C, Brennan M, Palaniswami M, Voss A." Poincaré Plot Methods for Heart Rate Variability Analysis." *Springer New York, NY*; (2013). ISBN: 978-1-4614-7374-9.

35- Singh D, Singh B. "Investigating the impact of data normalization on classification performance." *Applied Soft Computing* 97, 105524, (2020). https://doi.org/10.1016/j.asoc.2019.105524

36- Barahimi, S., Einalou, Z., & Dadgostar, M. "Evaluation of hemodynamic response function during mental arithmetic task in fNIRS data using GLM method", *Neuroscience Informatics*, 1 (1-2), 100004, (2021). https://doi.org/10.1016/j.neuri.2021.100004

37- Liu S. "Applying antagonistic activation pattern to the single-trial classification of mental arithmetic." *Heliyon*; 8:e11102, (2022)

38- Guo Z, Chen F. "Impacts of simplifying articulation movements imagery to speech imagery BCI performance." *J. Neural Eng*. (2023) (in press) https://doi.org/10.1088/1741-2552/acb232

39- Acharya U.R, Faust O, Kannathal N, Chua T, Laxminarayan S. "Non-linear analysis of EEG signals at various sleep stages." *Computer Methods and Programs in Biomedicine*; 80(1): 37-45, (2006). https://doi.org/10.1016/j.cmpb.2005.06.011.

40- Kim G-W, Ju C-Y, Seok H, Lee D-H. "Adaptive Stacking Ensemble Techniques for Early Severity Classification of COVID-19 Patients." *Applied Sciences*.; 14(7):2715, (2024). https://doi.org/10.3390/app14072715

41- Zhang X, Long K, Wang N, Zhang J, Lei H. "Synchronous measurements of prefrontal activity and pulse rate variability during online video game playing with functional near-infrared spectroscopy." *Journal of Innovative Optical Health Sciences*; 16(06): 2340005, (2023). https://doi.org/10.1142/S1793545823400059